Observation of the decay $\bar{B}^0 \to \Lambda_c^+ \bar{p} \pi^0$

B. Aubert,[1] Y. Karyotakis,[1] J. P. Lees,[1] V. Poireau,[1] E. Prencipe,[1] X. Prudent,[1] V. Tisserand,[1] J. Garra Tico,[2] E. Grauges,[2] M. Martinelli,[3a,3b] A. Palano,[3a,3b] M. Pappagallo,[3a,3b] G. Eigen,[4] B. Stugu,[4] L. Sun,[4] M. Battaglia,[5] D. N. Brown,[5] B. Hooberman,[5] L. T. Kerth,[5] Yu. G. Kolomensky,[5] G. Lynch,[5] I. L. Osipenkov,[5] K. Tackmann,[5] T. Tanabe,[5] C. M. Hawkes,[6] N. Soni,[6] A. T. Watson,[6] H. Koch,[7] T. Schroeder,[7] D. J. Asgeirsson,[8] C. Hearty,[8] T. S. Mattison,[8] J. A. McKenna,[8] M. Barrett,[9] A. Khan,[9] A. Randle-Conde,[9] V. E. Blinov,[10] A. D. Bukin,[10,*] A. R. Buzykaev,[10] V. P. Druzhinin,[10] V. B. Golubev,[10] A. P. Onuchin,[10] S. I. Serednyakov,[10] Yu. I. Skovpen,[10] E. P. Solodov,[10] K. Yu. Todyshev,[10] M. Bondioli,[11] S. Curry,[11] I. Eschrich,[11] D. Kirkby,[11] A. J. Lankford,[11] P. Lund,[11] M. Mandelkern,[11] E. C. Martin,[11] D. P. Stoker,[11] H. Atmacan,[12] J. W. Gary,[12] F. Liu,[12] O. Long,[12] G. M. Vitug,[12] Z. Yasin,[12] V. Sharma,[13] C. Campagnari,[14] T. M. Hong,[14] D. Kovalskyi,[14] M. A. Mazur,[14] J. D. Richman,[14] T. W. Beck,[15] A. M. Eisner,[15] C. A. Heusch,[15] J. Kroseberg,[15] W. S. Lockman,[15] A. J. Martinez,[15] T. Schalk,[15] B. A. Schumm,[15] A. Seiden,[15] L. Wang,[15] L. O. Winstrom,[15] C. H. Cheng,[16] D. A. Doll,[16] B. Echenard,[16] F. Fang,[16] D. G. Hitlin,[16] I. Narsky,[16] P. Ongmongkolkul,[16] T. Piatenko,[16] F. C. Porter,[16] R. Andreassen,[17] G. Mancinelli,[17] B. T. Meadows,[17] K. Mishra,[17] M. D. Sokoloff,[17] P. C. Bloom,[18] W. T. Ford,[18] A. Gaz,[18] J. F. Hirschauer,[18] M. Nagel,[18] U. Nauenberg,[18] J. G. Smith,[18] S. R. Wagner,[18] R. Ayad,[19,†] W. H. Toki,[19] E. Feltresi,[20] A. Hauke,[20] H. Jasper,[20] T. M. Karbach,[20] J. Merkel,[20] A. Petzold,[20] B. Spaan,[20] K. Wacker,[20] M. J. Kobel,[21] R. Nogowski,[21] K. R. Schubert,[21] R. Schwierz,[21] D. Bernard,[22] E. Latour,[22] M. Verderi,[22] P. J. Clark,[23] S. Playfer,[23] J. E. Watson,[23] M. Andreotti,[24a,24b] D. Bettoni,[24a] C. Bozzi,[24a] R. Calabrese,[24a,24b] A. Cecchi,[24a,24b] G. Cibinetto,[24a,24b] E. Fioravanti,[24a,24b] P. Franchini,[24a,24b] E. Luppi,[24a,24b] M. Munerato,[24a,24b] M. Negrini,[24a,24b] A. Petrella,[24a,24b] L. Piemontese,[24a] V. Santoro,[24a,24b] R. Baldini-Ferroli,[25] A. Calcaterra,[25] R. de Sangro,[25] G. Finocchiaro,[25] S. Pacetti,[25] P. Patteri,[25] I. M. Peruzzi,[25,‡] M. Piccolo,[25] M. Rama,[25] A. Zallo,[25] R. Contri,[26a,26b] E. Guido,[26a,26b] M. Lo Vetere,[26a,26b] M. R. Monge,[26a,26b] S. Passaggio,[26a] C. Patrignani,[26a,26b] E. Robutti,[26a] S. Tosi,[26a,26b] M. Morii,[27] A. Adametz,[28] J. Marks,[28] S. Schenk,[28] U. Uwer,[28] F. U. Bernlochner,[29] H. M. Lacker,[29] T. Lueck,[29] A. Volk,[29] P. D. Dauncey,[30] M. Tibbetts,[30] P. K. Behera,[31] M. J. Charles,[31] U. Mallik,[31] J. Cochran,[32] H. B. Crawley,[32] L. Dong,[32] V. Eyges,[32] W. T. Meyer,[32] S. Prell,[32] E. I. Rosenberg,[32] A. E. Rubin,[32] Y. Y. Gao,[33] A. V. Gritsan,[33] Z. J. Guo,[33] N. Arnaud,[34] A. D'Orazio,[34] M. Davier,[34] D. Derkach,[34] J. Firmino da Costa,[34] G. Grosdidier,[34] F. Le Diberder,[34] V. Lepeltier,[34] A. M. Lutz,[34] B. Malaescu,[34] P. Roudeau,[34] M. H. Schune,[34] J. Serrano,[34] V. Sordini,[34,§] A. Stocchi,[34] G. Wormser,[34] D. J. Lange,[35] D. M. Wright,[35] I. Bingham,[36] J. P. Burke,[36] C. A. Chavez,[36] J. R. Fry,[36] E. Gabathuler,[36] R. Gamet,[36] D. E. Hutchcroft,[36] D. J. Payne,[36] C. Touramanis,[36] A. J. Bevan,[37] C. K. Clarke,[37] F. Di Lodovico,[37] R. Sacco,[37] M. Sigamani,[37] G. Cowan,[38] S. Paramesvaran,[38] A. C. Wren,[38] D. N. Brown,[39] C. L. Davis,[39] A. G. Denig,[40] M. Fritsch,[40] W. Gradl,[40] A. Hafner,[40] K. E. Alwyn,[41] D. Bailey,[41] R. J. Barlow,[41] G. Jackson,[41] G. D. Lafferty,[41] T. J. West,[41] J. I. Yi,[41] J. Anderson,[42] C. Chen,[42] A. Jawahery,[42] D. A. Roberts,[42] G. Simi,[42] J. M. Tuggle,[42] C. Dallapiccola,[43] E. Salvati,[43] R. Cowan,[44] D. Dujmic,[44] P. H. Fisher,[44] S. W. Henderson,[44] G. Sciolla,[44] M. Spitznagel,[44] R. K. Yamamoto,[44] M. Zhao,[44] P. M. Patel,[45] S. H. Robertson,[45] M. Schram,[45] P. Biassoni,[46a,46b] A. Lazzaro,[46a,46b] V. Lombardo,[46a] F. Palombo,[46a,46b] S. Stracka,[46a,46b] L. Cremaldi,[47] R. Godang,[47,||] R. Kroeger,[47] P. Sonnek,[47] D. J. Summers,[47] H. W. Zhao,[47] X. Nguyen,[48] M. Simard,[48] P. Taras,[48] H. Nicholson,[49] G. De Nardo,[50a,50b] L. Lista,[50a] D. Monorchio,[50a,50b] G. Onorato,[50a,50b] C. Sciacca,[50a,50b] G. Raven,[51] H. L. Snoek,[51] C. P. Jessop,[52] K. J. Knoepfel,[52] J. M. LoSecco,[52] W. F. Wang,[52] L. A. Corwin,[53] K. Honscheid,[53] H. Kagan,[53] R. Kass,[53] J. P. Morris,[53] A. M. Rahimi,[53] S. J. Sekula,[53] N. L. Blount,[54] J. Brau,[54] R. Frey,[54] O. Igonkina,[54] J. A. Kolb,[54] M. Lu,[54] R. Rahmat,[54] N. B. Sinev,[54] D. Strom,[54] J. Strube,[54] E. Torrence,[54] G. Castelli,[55a,55b] N. Gagliardi,[55a,55b] M. Margoni,[55a,55b] M. Morandin,[55a] M. Posocco,[55a] M. Rotondo,[55a] F. Simonetto,[55a,55b] R. Stroili,[55a,55b] C. Voci,[55a,55b] P. del Amo Sanchez,[56] E. Ben-Haim,[56] G. R. Bonneaud,[56] H. Briand,[56] J. Chauveau,[56] O. Hamon,[56] Ph. Leruste,[56] G. Marchiori,[56] J. Ocariz,[56] A. Perez,[56] J. Prendki,[56] S. Sitt,[56] L. Gladney,[57] M. Biasini,[58a,58b] E. Manoni,[58a,58b] C. Angelini,[59a,59b] G. Batignani,[59a,59b] S. Bettarini,[59a,59b] G. Calderini,[59a,59b,¶] M. Carpinelli,[59a,59b,**] A. Cervelli,[59a,59b] F. Forti,[59a,59b] M. A. Giorgi,[59a,59b] A. Lusiani,[59a,59c] M. Morganti,[59a,59b] N. Neri,[59a,59b] E. Paoloni,[59a,59b] G. Rizzo,[59a,59b] J. J. Walsh,[59a] D. Lopes Pegna,[60] C. Lu,[60] J. Olsen,[60] A. J. S. Smith,[60] A. V. Telnov,[60] F. Anulli,[61a] E. Baracchini,[61a,61b] G. Cavoto,[61a] R. Faccini,[61a,61b] F. Ferrarotto,[61a] F. Ferroni,[61a,61b] M. Gaspero,[61a,61b] P. D. Jackson,[61a] L. Li Gioi,[61a] M. A. Mazzoni,[61a] S. Morganti,[61a] G. Piredda,[61a] F. Renga,[61a,61b] C. Voena,[61a] M. Ebert,[62] T. Hartmann,[62] H. Schröder,[62] R. Waldi,[62] T. Adye,[63] B. Franek,[63] E. O. Olaiya,[63] F. F. Wilson,[63] S. Emery,[64] L. Esteve,[64] G. Hamel de Monchenault,[64] W. Kozanecki,[64] G. Vasseur,[64] Ch. Yèche,[64] M. Zito,[64] M. T. Allen,[65] D. Aston,[65] D. J. Bard,[65] R. Bartoldus,[65] J. F. Benitez,[65] R. Cenci,[65] J. P. Coleman,[65] M. R. Convery,[65] J. C. Dingfelder,[65] J. Dorfan,[65] G. P. Dubois-Felsmann,[65] W. Dunwoodie,[65] R. C. Field,[65]

M. Franco Sevilla,[65] B. G. Fulsom,[65] A. M. Gabareen,[65] M. T. Graham,[65] P. Grenier,[65] C. Hast,[65] W. R. Innes,[65]
J. Kaminski,[65] M. H. Kelsey,[65] H. Kim,[65] P. Kim,[65] M. L. Kocian,[65] D. W. G. S. Leith,[65] S. Li,[65] B. Lindquist,[65] S. Luitz,[65]
V. Luth,[65] H. L. Lynch,[65] D. B. MacFarlane,[65] H. Marsiske,[65] R. Messner,[65,*] D. R. Muller,[65] H. Neal,[65] S. Nelson,[65]
C. P. O'Grady,[65] I. Ofte,[65] M. Perl,[65] B. N. Ratcliff,[65] A. Roodman,[65] A. A. Salnikov,[65] R. H. Schindler,[65] J. Schwiening,[65]
A. Snyder,[65] D. Su,[65] M. K. Sullivan,[65] K. Suzuki,[65] S. K. Swain,[65] J. M. Thompson,[65] J. Va'vra,[65] A. P. Wagner,[65]
M. Weaver,[65] C. A. West,[65] W. J. Wisniewski,[65] M. Wittgen,[65] D. H. Wright,[65] H. W. Wulsin,[65] A. K. Yarritu,[65]
C. C. Young,[65] V. Ziegler,[65] X. R. Chen,[66] H. Liu,[66] W. Park,[66] M. V. Purohit,[66] R. M. White,[66] J. R. Wilson,[66] M. Bellis,[67]
P. R. Burchat,[67] A. J. Edwards,[67] T. S. Miyashita,[67] S. Ahmed,[68] M. S. Alam,[68] J. A. Ernst,[68] B. Pan,[68] M. A. Saeed,[68]
S. B. Zain,[68] A. Soffer,[69] S. M. Spanier,[70] B. J. Wogsland,[70] R. Eckmann,[71] J. L. Ritchie,[71] A. M. Ruland,[71]
C. J. Schilling,[71] R. F. Schwitters,[71] B. C. Wray,[71] B. W. Drummond,[72] J. M. Izen,[72] X. C. Lou,[72] F. Bianchi,[73a,73b]
D. Gamba,[73a,73b] M. Pelliccioni,[73a,73b] M. Bomben,[74a,74b] L. Bosisio,[74a,74b] C. Cartaro,[74a,74b] G. Della Ricca,[74a,74b]
L. Lanceri,[74a,74b] L. Vitale,[74a,74b] V. Azzolini,[75] N. Lopez-March,[75] F. Martinez-Vidal,[75] D. A. Milanes,[75] A. Oyanguren,[75]
J. Albert,[76] Sw. Banerjee,[76] B. Bhuyan,[76] H. H. F. Choi,[76] K. Hamano,[76] G. J. King,[76] R. Kowalewski,[76] M. J. Lewczuk,[76]
I. M. Nugent,[76] J. M. Roney,[76] R. J. Sobie,[76] T. J. Gershon,[77] P. F. Harrison,[77] J. Ilic,[77] T. E. Latham,[77]
G. B. Mohanty,[77] E. M. T. Puccio,[77] H. R. Band,[78] X. Chen,[78] S. Dasu,[78] K. T. Flood,[78] Y. Pan,[78] R. Prepost,[78]
C. O. Vuosalo,[78] and S. L. Wu[78]

(*BABAR* Collaboration)

[1]*Laboratoire d'Annecy-le-Vieux de Physique des Particules (LAPP), Université de Savoie,
CNRS/IN2P3, F-74941 Annecy-Le-Vieux, France*
[2]*Universitat de Barcelona, Facultat de Fisica, Departament ECM, E-08028 Barcelona, Spain*
[3a]*INFN Sezione di Bari, I-70126 Bari, Italy*
[3b]*Dipartimento di Fisica, Università di Bari, I-70126 Bari, Italy*
[4]*University of Bergen, Institute of Physics, N-5007 Bergen, Norway*
[5]*Lawrence Berkeley National Laboratory and University of California, Berkeley, California 94720, USA*
[6]*University of Birmingham, Birmingham, B15 2TT, United Kingdom*
[7]*Ruhr Universität Bochum, Institut für Experimentalphysik 1, D-44780 Bochum, Germany*
[8]*University of British Columbia, Vancouver, British Columbia, Canada V6T 1Z1*
[9]*Brunel University, Uxbridge, Middlesex UB8 3PH, United Kingdom*
[10]*Budker Institute of Nuclear Physics, Novosibirsk 630090, Russia*
[11]*University of California at Irvine, Irvine, California 92697, USA*
[12]*University of California at Riverside, Riverside, California 92521, USA*
[13]*University of California at San Diego, La Jolla, California 92093, USA*
[14]*University of California at Santa Barbara, Santa Barbara, California 93106, USA*
[15]*University of California at Santa Cruz, Institute for Particle Physics, Santa Cruz, California 95064, USA*
[16]*California Institute of Technology, Pasadena, California 91125, USA*
[17]*University of Cincinnati, Cincinnati, Ohio 45221, USA*
[18]*University of Colorado, Boulder, Colorado 80309, USA*
[19]*Colorado State University, Fort Collins, Colorado 80523, USA*
[20]*Technische Universität Dortmund, Fakultät Physik, D-44221 Dortmund, Germany*
[21]*Technische Universität Dresden, Institut für Kern- und Teilchenphysik, D-01062 Dresden, Germany*
[22]*Laboratoire Leprince-Ringuet, CNRS/IN2P3, Ecole Polytechnique, F-91128 Palaiseau, France*
[23]*University of Edinburgh, Edinburgh EH9 3JZ, United Kingdom*
[24a]*INFN Sezione di Ferrara, I-44100 Ferrara, Italy*
[24b]*Dipartimento di Fisica, Università di Ferrara, I-44100 Ferrara, Italy*
[25]*INFN Laboratori Nazionali di Frascati, I-00044 Frascati, Italy*
[26a]*INFN Sezione di Genova, I-16146 Genova, Italy*
[26b]*Dipartimento di Fisica, Università di Genova, I-16146 Genova, Italy*
[27]*Harvard University, Cambridge, Massachusetts 02138, USA*
[28]*Universität Heidelberg, Physikalisches Institut, Philosophenweg 12, D-69120 Heidelberg, Germany*
[29]*Humboldt-Universität zu Berlin, Institut für Physik, Newtonstr. 15, D-12489 Berlin, Germany*
[30]*Imperial College London, London, SW7 2AZ, United Kingdom*
[31]*University of Iowa, Iowa City, Iowa 52242, USA*
[32]*Iowa State University, Ames, Iowa 50011-3160, USA*
[33]*Johns Hopkins University, Baltimore, Maryland 21218, USA*

[34]Laboratoire de l'Accélérateur Linéaire, IN2P3/CNRS et Université Paris-Sud 11,
Centre Scientifique d'Orsay, B. P. 34, F-91898 Orsay Cedex, France
[35]Lawrence Livermore National Laboratory, Livermore, California 94550, USA
[36]University of Liverpool, Liverpool L69 7ZE, United Kingdom
[37]Queen Mary, University of London, London, E1 4NS, United Kingdom
[38]University of London, Royal Holloway and Bedford New College, Egham, Surrey TW20 0EX, United Kingdom
[39]University of Louisville, Louisville, Kentucky 40292, USA
[40]Johannes Gutenberg-Universität Mainz, Institut für Kernphysik, D-55099 Mainz, Germany
[41]University of Manchester, Manchester M13 9PL, United Kingdom
[42]University of Maryland, College Park, Maryland 20742, USA
[43]University of Massachusetts, Amherst, Massachusetts 01003, USA
[44]Massachusetts Institute of Technology, Laboratory for Nuclear Science, Cambridge, Massachusetts 02139, USA
[45]McGill University, Montréal, Québec, Canada H3A 2T8
[46a]INFN Sezione di Milano, I-20133 Milano, Italy
[46b]Dipartimento di Fisica, Università di Milano, I-20133 Milano, Italy
[47]University of Mississippi, University, Mississippi 38677, USA
[48]Université de Montréal, Physique des Particules, Montréal, Québec, Canada H3C 3J7
[49]Mount Holyoke College, South Hadley, Massachusetts 01075, USA
[50a]INFN Sezione di Napoli, I-80126 Napoli, Italy
[50b]Dipartimento di Scienze Fisiche, Università di Napoli Federico II, I-80126 Napoli, Italy
[51]NIKHEF, National Institute for Nuclear Physics and High Energy Physics, NL-1009 DB Amsterdam, The Netherlands
[52]University of Notre Dame, Notre Dame, Indiana 46556, USA
[53]Ohio State University, Columbus, Ohio 43210, USA
[54]University of Oregon, Eugene, Oregon 97403, USA
[55a]INFN Sezione di Padova, I-35131 Padova, Italy
[55b]Dipartimento di Fisica, Università di Padova, I-35131 Padova, Italy
[56]Laboratoire de Physique Nucléaire et de Hautes Energies, IN2P3/CNRS, Université Pierre et Marie Curie-Paris6,
Université Denis Diderot-Paris7, F-75252 Paris, France
[57]University of Pennsylvania, Philadelphia, Pennsylvania 19104, USA
[58a]INFN Sezione di Perugia, I-06100 Perugia, Italy
[58b]Dipartimento di Fisica, Università di Perugia, I-06100 Perugia, Italy
[59a]INFN Sezione di Pisa, I-56127 Pisa, Italy
[59b]Dipartimento di Fisica, Università di Pisa, I-56127 Pisa, Italy
[59c]Scuola Normale Superiore di Pisa, I-56127 Pisa, Italy
[60]Princeton University, Princeton, New Jersey 08544, USA
[61a]INFN Sezione di Roma, I-00185 Roma, Italy
[61b]Dipartimento di Fisica, Università di Roma La Sapienza, I-00185 Roma, Italy
[62]Universität Rostock, D-18051 Rostock, Germany
[63]Rutherford Appleton Laboratory, Chilton, Didcot, Oxon, OX11 0QX, United Kingdom
[64]CEA, Irfu, SPP, Centre de Saclay, F-91191 Gif-sur-Yvette, France
[65]SLAC National Accelerator Laboratory, Stanford, California 94309 USA
[66]University of South Carolina, Columbia, South Carolina 29208, USA
[67]Stanford University, Stanford, California 94305-4060, USA
[68]State University of New York, Albany, New York 12222, USA
[69]Tel Aviv University, School of Physics and Astronomy, Tel Aviv, 69978, Israel
[70]University of Tennessee, Knoxville, Tennessee 37996, USA
[71]University of Texas at Austin, Austin, Texas 78712, USA
[72]University of Texas at Dallas, Richardson, Texas 75083, USA
[73a]INFN Sezione di Torino, I-10125 Torino, Italy
[73b]Dipartimento di Fisica Sperimentale, Università di Torino, I-10125 Torino, Italy
[74a]INFN Sezione di Trieste, I-34127 Trieste, Italy
[74b]Dipartimento di Fisica, Università di Trieste, I-34127 Trieste, Italy

[*]Deceased.
[†]Now at Temple University, Philadelphia, Pennsylvania 19122, USA.
[‡]Also with Università di Perugia, Dipartimento di Fisica, Perugia, Italy.
[§]Also with Università di Roma La Sapienza, I-00185 Roma, Italy.
[‖]Now at University of South Alabama, Mobile, Alabama 36688, USA.
[¶]Also with Laboratoire de Physique Nucléaire et de Hautes Energies, IN2P3/CNRS, Université Pierre et Marie Curie-Paris6, Université Denis Diderot-Paris7, F-75252 Paris, France.
[**]Also with Università di Sassari, Sassari, Italy.

^{75}*IFIC, Universitat de Valencia-CSIC, E-46071 Valencia, Spain*
^{76}*University of Victoria, Victoria, British Columbia, Canada V8W 3P6*
^{77}*Department of Physics, University of Warwick, Coventry CV4 7AL, United Kingdom*
^{78}*University of Wisconsin, Madison, Wisconsin 53706, USA*

In a sample of 467×10^6 $B\bar{B}$ pairs collected with the *BABAR* detector at the PEP-II collider at SLAC we have observed the decay $\bar{B}^0 \to \Lambda_c^+ \bar{p} \pi^0$ and measured the branching fraction to be $(1.94 \pm 0.17 \pm 0.14 \pm 0.50) \times 10^{-4}$, where the uncertainties are statistical, systematic, and the uncertainty on the $\Lambda_c^+ \to pK^-\pi^+$ branching fraction, respectively. We determine an upper limit of 1.5×10^{-6} at 90% C.L. for the product branching fraction $\mathcal{B}(\bar{B}^0 \to \Sigma_c^+(2455)\bar{p}) \times \mathcal{B}(\Lambda_c^+ \to pK^-\pi^+)$. Furthermore, we observe an enhancement at the threshold of the invariant mass of the baryon-antibaryon pair.

Although approximately 7% of *B*-meson decays have baryons in the final state, presently the sum of all measured branching fractions of exclusive baryonic *B* decays is only about 1% [1]. *B* mesons decay dominantly via $b \to c$ transitions, hence decays to baryons should be dominated by charm baryon production or a charmed meson accompanied by noncharmed baryons. Both types of decays have been observed [2,3], and are found to have comparable branching fractions for decays to final states with the same multiplicity.

In baryonic *B* decays and in baryon production in general, enhancements at the threshold for the baryon-antibaryon invariant mass have been observed [3,4]. This may indicate resonances near threshold or another mechanism for enhanced production of baryon-antibaryon pairs. This threshold enhancement may also explain the increase in branching fraction with final-state multiplicity and the apparent suppression of two-body decays to baryons [1,5].

The mechanisms of baryon production in heavy meson decays are poorly understood, and studies of exclusive decays may provide insight into different decay mechanisms. As will be discussed below, isospin relations will also help distinguish different primary processes.

In this paper, we present a study of the decay $\bar{B}^0 \to \Lambda_c^+ \bar{p} \pi^0$ [6] and measure its branching fraction. The CLEO collaboration previously set an upper limit of $\mathcal{B}(\bar{B}^0 \to \Lambda_c^+ \bar{p} \pi^0) < 5.9 \times 10^{-4}$ based on an integrated luminosity of 2.39 fb^{-1} [7]. For the isospin-related decay, $B^- \to \Lambda_c^+ \bar{p} \pi^-$, several measurements of the branching fraction have been performed [8,9]. The recent *BABAR* measurement gives $(3.38 \pm 0.12 \pm 0.12 \pm 0.88) \times 10^{-4}$ [10], a value that is significantly higher than earlier measurements (4.3σ deviation). The last and dominant error is due to the uncertainty in the $\Lambda_c^+ \to pK^-\pi^+$ branching fraction, common to all measurements.

While the $B^- \to \Lambda_c^+ \bar{p} \pi^-$ final-state can only have an isospin I of 3/2, $\bar{B}^0 \to \Lambda_c^+ \bar{p} \pi^0$ can also have $I = 1/2$. If both decays proceed via the same weak decay mechanism, $I = 3/2$, the ratio of the partial decay widths of $\bar{B}^0$ to B^- should be 2/3. However, it is also possible that the decay mechanisms are different. Thus a deviation of the ratio of

partial decay widths from 2/3 would suggest a contribution from the $I = 1/2$ final-state to the $\bar{B}^0 \to \Lambda_c^+ \bar{p} \pi^0$ decay or a contribution from the decay process where the π^- is coming from the *W* in the $B^- \to \Lambda_c^+ \bar{p} \pi^-$ decay.

This analysis is based on a data set of about 426 fb^{-1} corresponding to 467×10^6 $B\bar{B}$ pairs. These data were collected with the *BABAR* detector at the PEP-II asymmetric-energy e^+e^- collider with a center-of-mass energy, $\sqrt{s}$, at the $\Upsilon(4S)$ resonance mass. An additional sample of 44.5 fb^{-1}, collected 40 MeV below the mass of the $\Upsilon(4S)$ resonance, are used to study the continuum background $e^+e^- \to q\bar{q}$, where $q = u, d, s$, or c.

The signal efficiency is determined using a detailed GEANT4 [11] Monte Carlo (MC) simulation of the *BABAR* detector that generates MC events uniformly in the $\Lambda_c^+ \bar{p} \pi^0$ phase space. MC events are also used to study the background contributions.

The *BABAR* detector is described in detail elsewhere [12]. Charged particles are distinguished and their momenta measured in the tracking system consisting of a five-layer double-sided silicon vertex tracker (SVT) and a 40-layer drift chamber (DCH). An internally reflecting ring imaging Cherenkov detector (DIRC) is also used to distinguish charged particles and a CsI(Tl) electromagnetic calorimeter (EMC) is used to detect photons.

Likelihood ratios based on information from SVT, DCH and DIRC are used to identify protons and kaons. The efficiency for the kaon selection is around 90% while the rate for misidentifying pions and protons as kaons varies between 5% and 10%, depending on track momentum. The identification efficiency for the proton selection is greater than 90% while the misidentification rate of identifying kaons and pions as protons varies between 3% and 15%, depending on track momentum.

Two photons are selected as electromagnetic showers in the EMC with the expected shape and are combined to form a π^0 candidate, where the photon with the lower energy must have an energy greater than 60 MeV, while the second photon must have an energy greater than 100 MeV. The invariant mass of the $\gamma\gamma$ combination is required to be between 120 MeV/c^2 and 145 MeV/c^2.

The Λ_c^+ candidates are reconstructed in the decay mode $\Lambda_c^+ \rightarrow pK^-\pi^+$, and a fit with geometric constraint applied to the common vertex must have a χ^2 probability greater than 0.1%. The invariant $pK^-\pi^+$ mass must be within 2.5σ of the fitted peak of the mass distribution, $2.276 < m(pK^-\pi^+) < 2.296$ GeV/c^2. The Λ_c^+ and π^0 candidates are then combined with a $\bar{p}$ candidate in a fit using kinematic constraints to form a $\bar{B}^0$ candidate. In the fit, the mass of the $pK^-\pi^+$ candidate is constrained to the mass of the Λ_c^+ and the mass of the $\gamma\gamma$ combination to the mass of the π^0 [1]. The χ^2 probability of this fit must be greater than 0.1%.

The analysis makes use of two almost independent kinematic variables, ΔE and m_{ES}, where $\Delta E = E_B^* - \sqrt{s}/2$ is the difference of the reconstructed energy E_B^* and half of $\sqrt{s}$ in the e^+e^- center-of-mass frame (CMS). The other variable is $m_{ES} = \sqrt{(s/2 + \mathbf{p_0} \cdot \mathbf{p_B})^2/E_0^2 - \mathbf{p_B^2}}$ where $(E_0, \mathbf{p_0})$ is the four momentum of the e^+e^- system and $\mathbf{p_B}$ is the B candidate momentum, both measured in the laboratory frame. The m_{ES} distribution for signal events peaks at the B mass and the distribution of ΔE for signal events is centered around zero. Candidates arising from other B decays, with more final-state particles, such as $\bar{B}^0 \rightarrow \Lambda_c^+ \bar{p}\pi^+\pi^-$, are shifted to negative values of ΔE. Conversely, candidates arising from B decays with fewer final-state particles, such as $\bar{B}^0 \rightarrow \Lambda_c^+ \bar{p}$, are shifted to positive values. To suppress these decays, only candidates with -50 MeV $< \Delta E < 40$ MeV are selected.

A considerable background comes from $B^- \rightarrow \Lambda_c^+ \bar{p}\pi^-$ decays, and, in particular, from the $B^- \rightarrow \Sigma_c^0(2455)\bar{p}$, $\Sigma_c^0(2455) \rightarrow \Lambda_c^+ \pi^-$ decays, in which the $\Lambda_c^+ \bar{p}$ pair from B^- decay is combined with a π^0 from the decay of the B^+ meson. To suppress this background, we reconstruct $B^- \rightarrow \Lambda_c^+ \bar{p}\pi^-$, and reject the event if $|\Delta E| < 50$ MeV and $m_{ES} > 5.27$ GeV/c^2 for such a B^- candidate, or if the condition 2400 MeV/$c^2 < m(\Lambda_c^+ \pi^-) < 2465$ MeV/c^2 is satisfied (veto cuts). These two requirements keep 98% of the signal, while they remove 85% of $B^- \rightarrow \Sigma_c^0(2455)\bar{p}$ events. The remaining 15% of the background events do not peak in the signal $\Delta E - m_{ES}$ region.

The continuum background is reduced by a requirement on the thrust value of the event $T < 0.75$, where we include both charged particles and photons in this calculation. The thrust is defined as

$$T = \frac{\sum_i |\hat{T} \cdot \mathbf{p}_i|}{\sum_i |\mathbf{p}_i|}, \tag{1}$$

where $\hat{T}$ is the thrust axis defined as the direction which maximizes the sum of the longitudinal momenta of the particles, and $\mathbf{p}_i$ the momentum vector of the i-th particle in the CMS. This selection keeps 83% of the signal but only 25% of the continuum background, as determined

from MC simulation and continuum data collected 40 MeV below the $\Upsilon(4S)$ energy.

To further reduce the background from continuum and $B\bar{B}$ events, mainly coming from $\gamma\gamma$ combinations of low energy, only one $\bar{B}^0$ candidate per event is selected. In events with more than one candidate (about 10% of the events), first the candidate(s) with the invariant mass $m(\gamma\gamma)$ closest to the π^0 nominal mass are selected. For events with multiple candidates containing the same π^0, the candidate with the $pK^-\pi^+$ mass closest to the nominal Λ_c mass is retained. If there are still multiple B candidates, the candidate with the highest probability of the kinematic vertex fit is used. Figure 1 shows a comparison between the ΔE distribution of candidates reconstructed in data and in signal MC events, in which signal events are obtained by a fit to the m_{ES} distribution in every ΔE bin, as described below.

The number of reconstructed signal candidates is determined from a binned χ^2 fit to the observed m_{ES} distribution shown in Fig. 2. The sum of two Gaussian distributions with different means is used to describe the signal. The parameters of the two Gaussians are fixed to the values obtained from a fit to signal MC events. The background is described by the function [13] $f_{bg} = n \times m_{ES}\sqrt{1 - (m_{ES}/m_0)^2} \times e^{-c(1-(m_{ES}/m_0)^2)}$, where $m_0 = 5.289$ GeV/c^2 is the kinematic end-point value, c a shape parameter left free in the fit, and n is the normalization. There are 273 ± 23 signal candidates seen in data and the significance of this observation is more than 10σ.

The number of produced signal events used to measure the branching fraction is determined by a fit to the efficiency-corrected m_{ES} distribution using the same parametrization as before. The events are weighted with the inverse of the efficiency as a function of the invariant mass
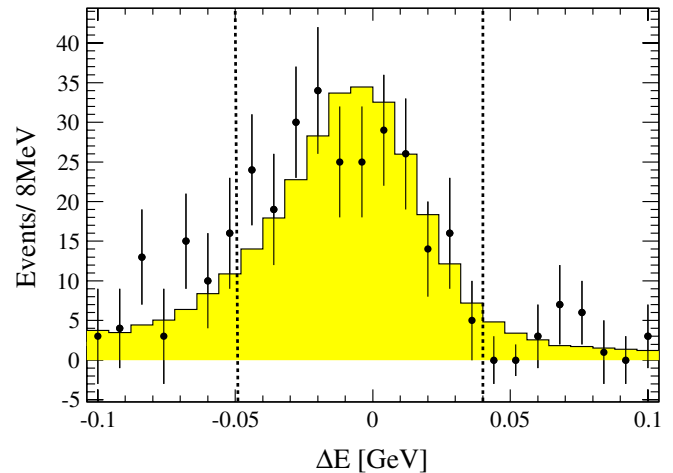

FIG. 1 (color online). ΔE distribution for data signal events after all selection cuts (data points) and signal MC events (histogram) normalized to the number of data signal events; signal events are obtained from binwise m_{ES} fits; dashed lines show the range used for m_{ES} distributions.
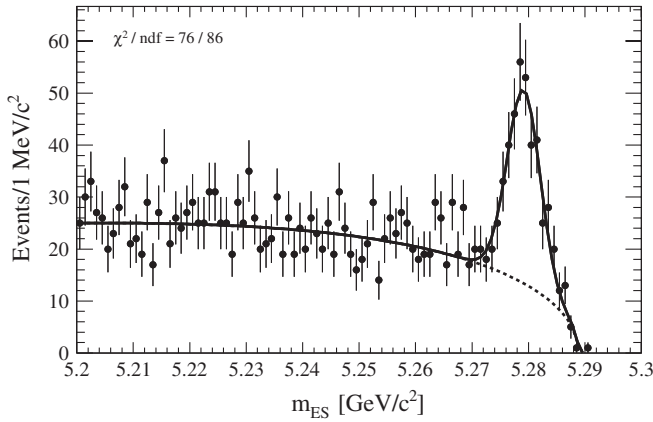
FIG. 2. Fitted m_{ES} distribution without efficiency correction (data points); the result of the fit (solid line) and the background estimate (dashed line) is shown.

$m(\Lambda_c^+ \pi^0)$. To compute the efficiency, the signal MC sample is divided in 10 intervals of $m(\Lambda_c^+ \pi^0)$. For each interval the m_{ES} distribution is fitted to extract the signal MC yield. The efficiency for each interval is computed dividing the yield by the number of events generated in this interval. The resulting efficiency distribution is then fitted by a 4th order polynomial. The averaged signal efficiency is 6.0%.

The weighted data m_{ES} distribution is shown in Fig. 3, and the fit found 4528 ± 403 signal events (N_{signal}). The branching fraction is then calculated as

$$\mathcal{B}(\bar{B}^0 \rightarrow \Lambda_c^+ \bar{p} \pi^0) = \frac{N_{\text{signal}}}{\mathcal{B}(\Lambda_c^+ \rightarrow pK^- \pi^+) \cdot 2N_{B^0\bar{B}^0}}$$
$$= (1.94 \pm 0.17) \times 10^{-4}, \qquad (2)$$

where the uncertainty is statistical only from the fit, and $\mathcal{B}(\Lambda_c^+ \rightarrow pK^- \pi^+) = (0.050 \pm 0.013)$ [1]. The quantity $N_{B^0\bar{B}^0} = (233.6 \pm 2.6) \times 10^6$ is the number of $B^0\bar{B}^0$ pairs and $\mathcal{B}(Y(4S) \rightarrow B^0\bar{B}^0) = 0.5$ is assumed.
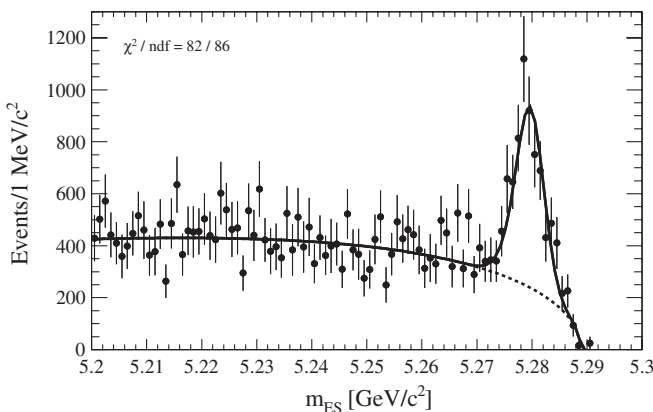

FIG. 3. Efficiency-corrected m_{ES} distribution for $\bar{B}^0 \rightarrow \Lambda_c^+ \bar{p} \pi^0$ (data points). The result of the fit (solid line) and the background estimate (dashed line) is shown.

To check for peaking background from other B decays and random $\gamma\gamma$ combinations, the analysis is repeated for selected samples without mass constraints on the π^0 and Λ_c^+ mass. The signal yields after subtraction of background obtained from the invariant mass distributions of the π^0 and Λ_c^+ are found to be consistent with the default analysis.

The systematic uncertainties are mainly derived from studies of data control samples and by comparison of data and MC events. The main systematic uncertainty arises from differences between data and MC events in the ΔE distribution seen in Fig. 1. The difference between the cut efficiency in MC and data, relative to the MC one, is used as the systematic uncertainty (4.6%). Other systematic uncertainties arise from the veto cuts (3.4%), the π^0 reconstruction efficiency (3.0%), the particle identification (1.2%), the number of $B^0\bar{B}^0$ pairs (1.1%) and the reconstruction efficiency of charged tracks (0.9%). To determine the uncertainty from the MC model we use to generate signal events, these signal events are reweighted depending on $m(\bar{p}\pi^0)$, and a new efficiency function is calculated. The data m_{ES} distribution is then corrected for reconstruction efficiencies with this function and fitted as before. The difference in the number of signal events we use as the systematic uncertainty of the specific MC model (2.2%). The systematic uncertainty due to the fit is determined by changing the cut-off value of the background function by 1 MeV/c^2 (0.50%). The individual contributions to the systematic uncertainty are added in quadrature, resulting in the total of 7.1%.

In Fig. 4, the measured $m(\Lambda_c^+ \bar{p})$ distribution is compared with a MC simulated one, generated with a phase space distribution for the decay to $\Lambda_c^+ \bar{p} \pi^0$ and normalized to the number of data events. To extract the signal distribution events, the m_{ES} distribution is fitted in every bin of $m(\Lambda_c^+ \bar{p})$. There is a clear difference in shape between data and simulation, with a clear enhancement at low mass, with
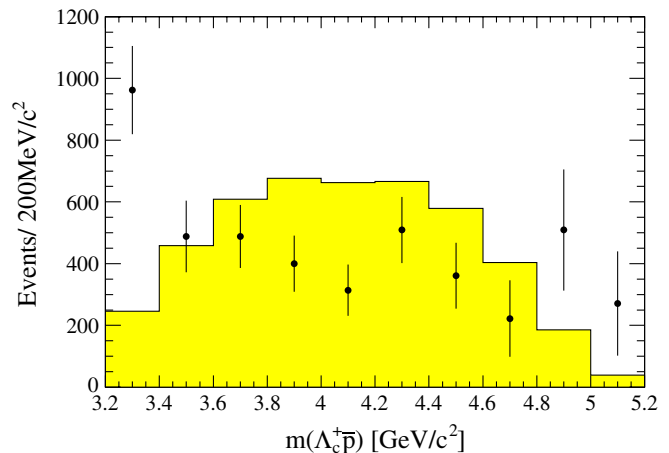

FIG. 4 (color online). Efficiency corrected distribution of the invariant mass $m(\Lambda_c^+ \bar{p})$; points are signal data events; histogram shows signal MC events assuming phase space distribution normalized to the number of data events.

a significance of 5σ for the first bin, assuming Gaussian statistics. Such an enhancement is seen in many other baryonic B decays and also in baryon production, such as $e^+ e^- \to \gamma \Lambda \bar{\Lambda}$ [14], which proceeds through different short-distance processes.

In Fig. 5, the invariant mass of the $\Lambda_c^+ \pi^0$ combination is shown, fitted by a Gaussian function for a possible $\Sigma_c^+(2455)$ signal and by the function $n \times (m(\Lambda_c^+ \pi^0) - [m(\Lambda_c^+) + m(\pi^0)])^c$ to describe the nonresonant fraction of the signal and background using a likelihood fit. The shape parameters for the Gaussian are fixed to the parameters obtained from simulated events. The fit returns $N_{\Sigma_c^+(2455)} = 3 \pm 3$ signal events. Therefore, there is no evidence for $\bar{B}^0 \to \Sigma_c^+(2455)\bar{p}$. The reconstruction efficiency for $\bar{B}^0 \to \Sigma_c^+(2455)\bar{p}$ is $(1.70 \pm 0.05)\%$. Integrating the likelihood function of the fit parameter $N_{\Sigma_c^+(2455)} \geq 0$, we obtain a Bayesian upper limit at 90% confidence level (C.L.) of $\mathcal{B}(\bar{B}^0 \to \Sigma_c^+(2455)\bar{p}) \times \mathcal{B}(\Lambda_c^+ \to K^- p \pi^+) < 1.5 \times 10^{-6}$.

In conclusion, we have observed the decay $\bar{B}^0 \to \Lambda_c^+ \bar{p} \pi^0$ and measured the branching fraction as:

$$\mathcal{B}(\bar{B}^0 \to \Lambda_c^+ \bar{p} \pi^0) = (1.94 \pm 0.17 \pm 0.14 \pm 0.50) \times 10^{-4},$$
(3)

where the uncertainties are statistical, systematic, and from the Λ_c^+ branching fraction, $\Lambda_c^+ \to pK^- \pi^+$. The ratio of the partial decay width measured here to the *BABAR* measurement of the decay $B^- \to \Lambda_c^+ \bar{p} \pi^-$ [10] is

$$\frac{\mathcal{B}(\bar{B}^0 \to \Lambda_c^+ \bar{p} \pi^0)}{\mathcal{B}(B^- \to \Lambda_c^+ \bar{p} \pi^-)} \times \frac{\tau_{B^-}}{\tau_{\bar{B}^0}} = 0.61 \pm 0.09,$$
(4)

where τ_{B^-} and $\tau_{\bar{B}^0}$ are the lifetimes of the B mesons. This ratio is consistent with the isospin expectation of $2/3$. Given that we do not have evidence for a $\bar{B}^0 \to \Sigma_c^+ \bar{p}$ contribution, we also compare our $\bar{B}^0 \to \Lambda_c^+ \bar{p} \pi^0$ measurement with only the nonresonant contribution to the $B^- \to \Lambda_c^+ \bar{p} \pi^-$ decay. We find

$$\frac{\mathcal{B}(\bar{B}^0 \to \Lambda_c^+ \bar{p} \pi^0)}{\mathcal{B}(B^- \to \Lambda_c^+ \bar{p} \pi^-)_{\text{nonresonant}}} \times \frac{\tau_{B^-}}{\tau_{\bar{B}^0}} = 0.80 \pm 0.11,$$
(5)

which is also consistent with the isospin expectation of $2/3$.

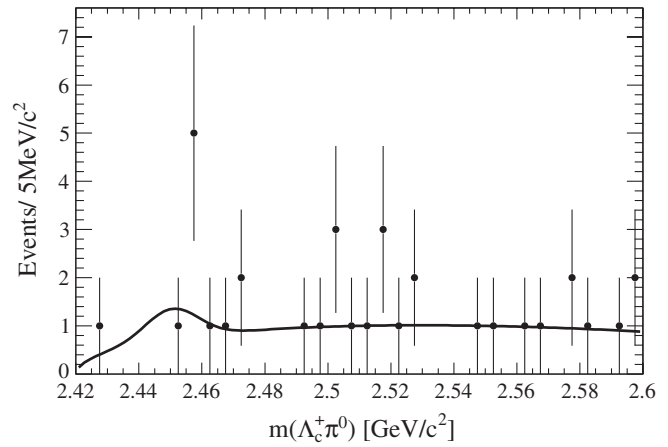For the resonant subchannel we calculate a 90% upper limit of

FIG. 5.   Distribution of the invariant mass of the $\Lambda_c^+ \pi^0$ system in the region where the $\Sigma_c^+(2455)$ resonance is expected; points are for data with $m_{\mathrm{ES}} > 5.272$ GeV/c^2, the curve shows the fit.

$$\mathcal{B}(\bar{B}^0 \to \Sigma_c^+(2455)\bar{p}) \times \mathcal{B}(\Lambda_c^+ \to K^- p \pi) < 1.5 \times 10^{-6}.$$
(6)

The 90% C.L. Bayesian upper limit for the ratio of the branching fractions $\mathcal{B}(\bar{B}^0 \to \Sigma_c^+(2455)\bar{p})$ and $B^- \to \Sigma_c^0(2455)\bar{p}$ [10] is

$$\frac{\mathcal{B}(\bar{B}^0 \to \Sigma_c^+(2455)\bar{p})}{\mathcal{B}(B^- \to \Sigma_c^0(2455)\bar{p})} \times \frac{\tau_{B^-}}{\tau_{\bar{B}^0}} < 0.73,$$
(7)

which we compute by integrating the likelihood profile for the ratio of branching fractions over the positive range. It is also consistent with the isospin expectation of $2/3$.

[1] C. Amsler *et al.* (Particle Data Group), Phys. Lett. B **667**, 1 (2008).

[2] K. Abe *et al.* (Belle Collaboration), Phys. Rev. Lett. **89**, 151802 (2002).

[3] B. Aubert *et al.* (*BABAR* Collaboration), Phys. Rev. D **74**, 051101 (2006).

[4] B. Aubert *et al.* (*BABAR* Collaboration), Phys. Rev. D **72**, 051101 (2005).

[5] W.-S. Hou and A. Soni, Phys. Rev. Lett. **86**, 4247 (2001).

[6] Throughout this paper charge conjugate modes are always

implied.

[7] X. Fu *et al.* (CLEO Collaboration), Phys. Rev. Lett. **79**, 3125 (1997).

[8] S. A. Dytman *et al.* (CLEO Collaboration), Phys. Rev. D **66**, 091101 (2002).

[9] N. Gabyshev *et al.* (Belle Collaboration), Phys. Rev. Lett. **97**, 242001 (2006).

[10] B. Aubert *et al.* (*BABAR* Collaboration), Phys. Rev. D **78**, 112003 (2008).

[11] S. Agostinelli *et al.* (GEANT4 Collaboration), Nucl. Instrum. Methods Phys. Res., Sect. A **506**, 250 (2003).

[12] B. Aubert *et al.* (*BABAR* Collaboration), Nucl. Instrum. Methods Phys. Res., Sect. A **479**, 1 (2002).

[13] H. Albrecht *et al.* (ARGUS Collaboration), Phys. Lett. B **241**, 278 (1990).

[14] B. Aubert *et al.* (*BABAR* Collaboration), Phys. Rev. D **76**, 092006 (2007).